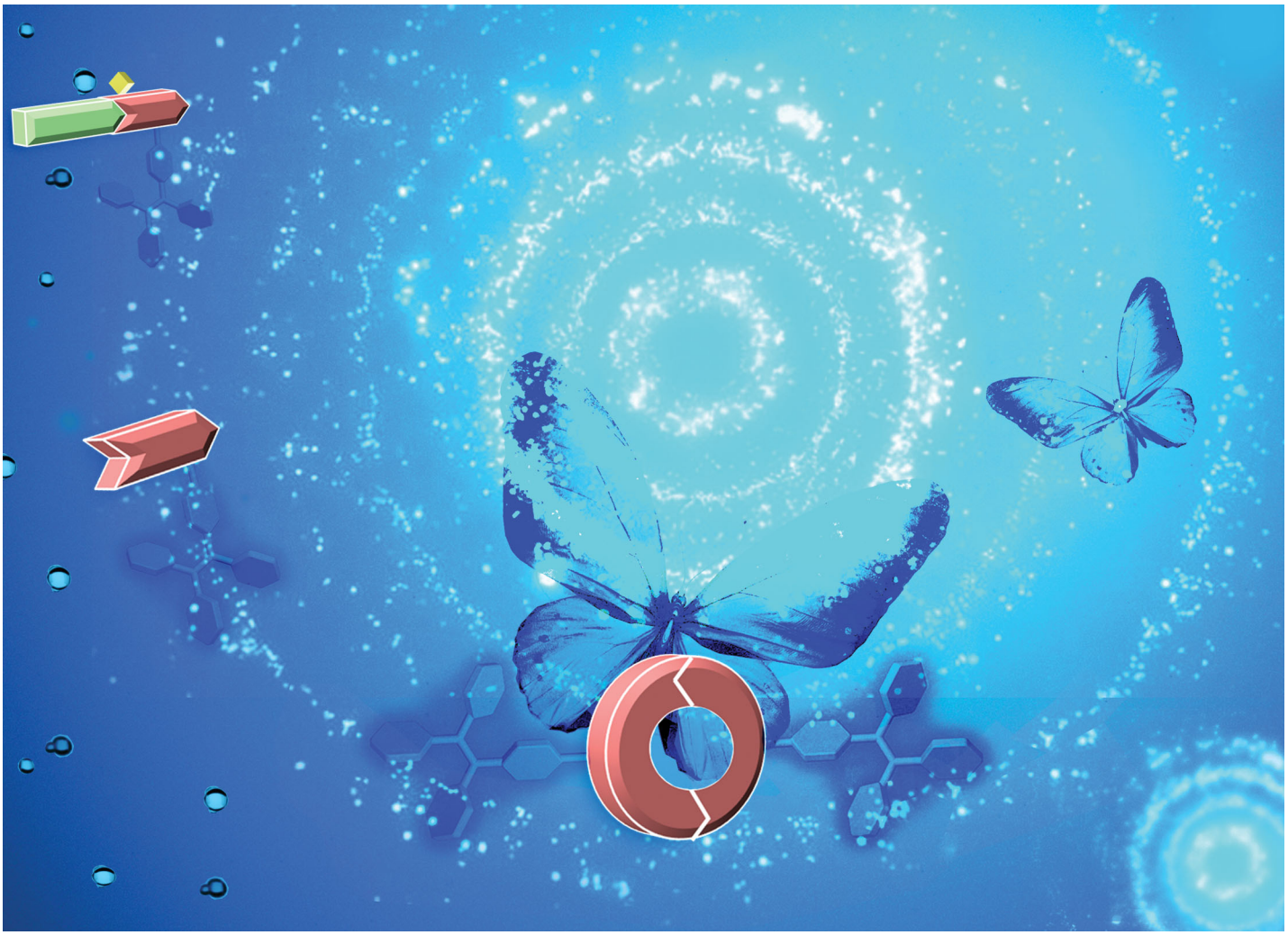

Showcasing research from the group of Professor Gaolin Liang at the Department of Chemistry, University of Science and Technology of China, China.

Dual aggregation-induced emission for enhanced fluorescence sensing of furin activity *in vitro* and in living cells

By integrating a biocompatible condensation reaction with an aggregation-induced emission (AIE) fluorogen, the Liang group developed a "smart" dual AIE probe for enhanced fluorescence sensing of furin activity *in vitro* and in living cells.

As featured in:

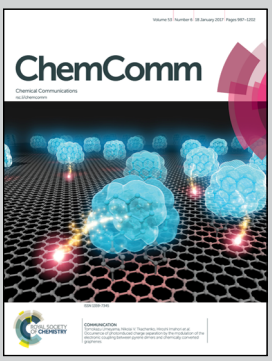

See Xiaomei Liu and Gaolin Liang, *Chem. Commun.*, 2017, **53**, 1037.

ROYAL SOCIETY OF CHEMISTRY

rsc.li/chemcomm

Registered charity number: 207890

ChemComm

COMMUNICATION

View Article Online
View Journal | View Issue

Cite this: *Chem. Commun.*, 2017, 53, 1037

Received 15th November 2016,
Accepted 12th December 2016

DOI: 10.1039/c6cc09106g

www.rsc.org/chemcomm

Dual aggregation-induced emission for enhanced fluorescence sensing of furin activity *in vitro* and in living cells†

Xiaomei Liu and Gaolin Liang*

The aggregation-induced emission (AIE) effect has recently been widely applied for biomarker sensing. But developing "smart" strategies to effectively aggregate the AIE fluorogen and additionally enhance the fluorescence emission remain challenging. In this work, by integrating a biocompatible condensation reaction with an AIE fluorogen, we rationally designed a "smart" dual AIE probe Ac-Arg-Val-Arg-Arg-Cys(StBu)-Lys(TPE)-CBT (1) for enhanced fluorescence sensing furin activity *in vitro* and in living cells. Compared with the single AIE probe Ac-Arg-Val-Arg-Arg-Lys(TPE)-OH (1-Ctrl) which also subjects to furin cleavage, fluorescence emissions of 1 were additionally enhanced 1.7 fold and 3.4 fold *in vitro* and in living cells, respectively. We envision that, in the near future, our "smart" strategy of enzyme-instructed dual AIE could be widely applied for sensing (or imaging) enzyme activity *in vitro* and even *in vivo* with dramatically enhanced sensitivity.

Enzymes are known as a class of natural proteins by which most biochemical processes are efficiently catalyzed in a controlled manner and with precise specificity.[1] The enzyme furin is a kind of trans-Golgi protein convertase that plays important roles in many diseases including Alzheimer's, Ebola fever, and cancer.[2] Specifically, furin was reported overexpressing in several cancers including carcinomas of the head and neck, non-small-cell lung carcinomas, and glioblastomas.[3] The peptide sequences Arg-X-Lys/Arg-Arg↓X (X can be any amino acid residue and ↓ indicates the cleavage site) were reported to be the preferential substrates for furin cleavage.[4] Based on the specific substrates, many probes have been developed for sensing (or imaging) furin activity with different modalities including fluorescence (FL),[5] magnetic resonance,[6] nuclear,[7] bioluminescence (BL),[8] *etc.* Among the above techniques, FL and BL have attracted much attention due to their simplicity, ease of operation, and needlessness of expensive instrumentation. BL almost does not have any background signal but the inexistence of luciferase in mammalian cells limits the applications of BL in rodents. Compared with FL "Turn-Off" probes, FL "Turn-On" probes are superior in the lower background signal and recently a FL "Turn-On" nanoprobe was successfully developed for furin detection *in vitro* and *in vivo*.[9]

Most of the FL "Turn-On" probes use the fluorescence resonance energy transfer (FRET) effect to turn "On" their FL. For instance, upon the cleavage of the linker by an enzyme, the quencher is separated from the fluorophore, thus turning "On" the FL of the probe.[10–13] However, the FL enhancement of a "Turn-On" probe sometimes was not as high as expected probably due to that, after the quencher left the probe, the solubility of the fluorophore in the solvent dramatically decreased which resulted in another aggregation-caused quenching (ACQ) of the fluorophore.[14] Unlike the ACQ fluorophores, aggregation-induced emission (AIE) fluorogens such as tetraphenylethylene (TPE) are nonemissive in the dissolved state but strongly emissive in the aggregate state, which is attributed to the restriction of intramolecular rotations (RIRs).[15] To date, a variety of AIE-based fluorogens have been developed for sensing the activities of various enzymes such as trypsin,[16] alkaline phosphatase,[17] and caspase.[18,19] Generally, the "Turn-On" FL of these AIE probes resulted from the direct aggregation of the fluorogens after enzyme cleavage (we call "Single AIE" in this work). Nevertheless, to the best of our knowledge, there was no report of further aggregation (we call "Dual AIE" in this work) of the AIE fluorogens, which would obviously result in an enhanced FL "Turn-On" for more efficient sensing (or imaging) of enzyme activity.

Recently, Rao and Liang developed a biocompatible click condensation reaction between the 1,2-aminothiol group of cysteine (Cys) and the cyano group of 2-cyanobenzothiazole (CBT) which can be controlled by pH, reduction, or protease for the self-assembly (or aggregation) of nanoparticles.[20,21] By conjugation of an imaging tag to the monomer, this CBT–Cys condensation reaction was successfully employed to self-assemble (or aggregate)

CAS Key Laboratory of Soft Matter Chemistry, Department of Chemistry, University of Science and Technology of China, 96 Jinzhai Road, Hefei, Anhui 230026, China. E-mail: gliang@ustc.edu.cn

† Electronic supplementary information (ESI) available: General methods; syntheses and characterization of TPE-COOH, **1**, **1-Scr**, and **1-Ctrl**; transmittance spectra; HPLC analyses; fluorescence spectra; DLS measurements; MTT assay of **1**, **1-Scr**, and **1-Ctrl**; time course fluorescence images of **1**-treated cells; Fig. S1–S27 and Tables S1–S3. See DOI: 10.1039/c6cc09106g

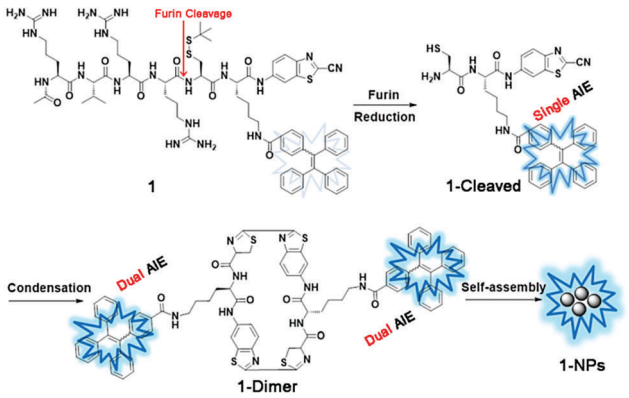

Scheme 1 Schematic illustration of furin-controlled dual aggregation-induced emission for enhanced fluorescence sensing of furin activity.

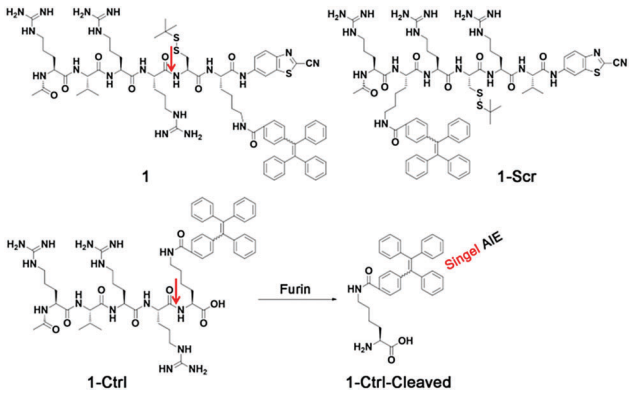

Fig. 1 Chemical structures of **1**, **1-Scr**, and **1-Ctrl**. Schematic illustration of **1-Ctrl** for furin cleavage. The red arrows indicate the furin cleavage sites.

nanoprobes to concentrate the signal for enhanced sensing (or imaging) of enzyme activity *in vitro* and *in vivo*.[22–24] Unluckily, if the tag was a conventional fluorophore, the aggregation of nanoparticles by this condensation reaction would result in ACQ of the FL and only subsequent disassembly of the nanoparticles could partially restore the FL for enzyme detection (or imaging).[9]

Inspired by above pioneering studies, in this work, we intended to integrate the AIE properties of a TPE molecule with a furin-controlled CBT–Cys condensation to dually aggregate the TPE fluorogen. Consequently, the "Dual AIE" effect could be realized for enhanced FL sensing and imaging of furin activity. To achieve this, as shown in Scheme 1, we rationally designed a probe Ac-Arg-Val-Arg-Arg-Cys(StBu)-Lys(TPE)-CBT (**1**) which contains the following components: an Ac-Arg-Val-Arg-Arg (RVRR) peptide sequence which not only improves the cellular uptake of the probe but also is the substrate for furin cleavage; a CBT motif and a disulfided Cys motif for CBT–Cys condensation; and a TPE motif conjugating to the side chain of a lysine (Lys) motif. As illustrated in Scheme 1, after **1** entering furin-overexpressing tumor cells (*e.g.*, MDA-MB-468 cells), its disulfide bond on the cysteine motifs is reduced by intracellular glutathione (GSH) and its RVRR peptide substrate is cleaved by furin to yield the reactive intermediate **1-Cleaved**. Theoretically, **1-Cleaved** is more hydrophobic than **1** and the conversion of **1** to **1-Cleaved** will lead to the first aggregation of the TPE fluorogen (*i.e.*, single AIE). Instantly, the free 1,2-aminothiol group and the cyano group on the CBT motif of **1-Cleaved** condense to yield the more hydrophobic dimer (*i.e.*, **1-Dimer**), which self-assembles (or aggregates) into the nanoparticles (*i.e.*, **1-NPs**) at (or near) the locations of activated furin (*i.e.* Golgi bodies), as demonstrated previously.[9,23] The conversion of **1-Cleaved** to **1-Dimer** and **1-NPs** will lead to further aggregation of the TPE fluorogen (*i.e.*, dual AIE) and thus its fluorescence is additionally enhanced. With this dual AIE strategy, furin activity in tumor cells could in turn be more sensitively detected (or imaged). To validate our hypothesis, a scrambled analog Ac-Arg-Lys(TPE)-Arg-Cys(StBu)-Arg-Val-CBT (**1-Scr**), which is insusceptible to furin cleavage (*i.e.*, no AIE effect), was synthesized for a parallel study (Fig. 1). As we mentioned above, **1-Cleaved** possesses the single AIE effect but it is a reactive intermediate and can hardly be captured. Thus, in this work, another control probe Ac-Arg-Val-Arg-Arg-Lys(TPE)-OH (**1-Ctrl**), which only subjects to furin cleavage but does not take the condensation reaction, possessing the single AIE effect was also synthesized for the proof of our concept (Fig. 1).

We began the study with the syntheses of **1**, **1-Scr**, and **1-Ctrl**. The syntheses are facile and straightforward (Schemes S1–S4 in the ESI†). Briefly, TPE-COOH was synthesized following the literature.[25] The peptide sequence Ac-Arg-Val-Arg-Arg-Cys(StBu)-Lys-OH (**A**) with protecting groups was synthesized using solid phase peptide synthesis (SPPS). The coupling of **A** with CBT in the presence of isobutyl chloroformate yielded **B** after high-performance liquid chromatography (HPLC) purification. The deprotection of **B** yielded **C** and coupling **C** with TPE-NHS ester yielded **1** after HPLC purification. The synthesis of **1-Scr** was similar to that of **1** except the peptide sequence was scrambled. **1-Ctrl** was obtained by the direct coupling of Ac-Arg-Val-Arg-Arg-Lys-OH with TPE-NHS ester after HPLC purification. The compounds were fully characterized using ^{1}H NMR, ^{13}C NMR, and mass spectrometry (MS) analyses (Fig. S1–S11 in the ESI†). After obtaining the pure compounds, we firstly investigated the AIE properties of the compounds in DMSO/H_2O mixtures. At DMSO fractions less than 50%, TPE-COOH exhibited obvious AIE properties with a fluorescence emission peak at 470 nm (Fig. S12 in the ESI†). The transmittance spectra of **1** in the DMSO/water mixtures indicated that at DMSO fractions more than 5%, **1** was totally dissolved in the mixture (Fig. S13A in the ESI†). Fluorescence emission spectra indicated that at DMSO fraction of 5%, while TPE-COOH had a strong emission at 470 nm, none of the compounds **1**, **1-Scr**, or **1-Ctrl** showed any emission at this wavelength (Fig. S13B in the ESI†). Thus, we chose the aqueous solution containing 5% DMSO as the solvent for the *in vitro* experiments below.

In order to qualitatively and quantitatively measure the enzymatic cleavage efficiency using HPLC, we used 100 μM of **1**, **1-Scr**, or **1-Ctrl** for the enzymatic assay. When dissolved in furin buffer containing 5% DMSO and 1 mM tris(2-carboxyethyl)-phosphine (TCEP) at pH 7.4, none of 100 μM **1**, **1-Scr**, or **1-Ctrl** solution showed detectable fluorescence emission at 470 nm (Fig. 2A and B and Fig. S14A in the ESI†). However, after the

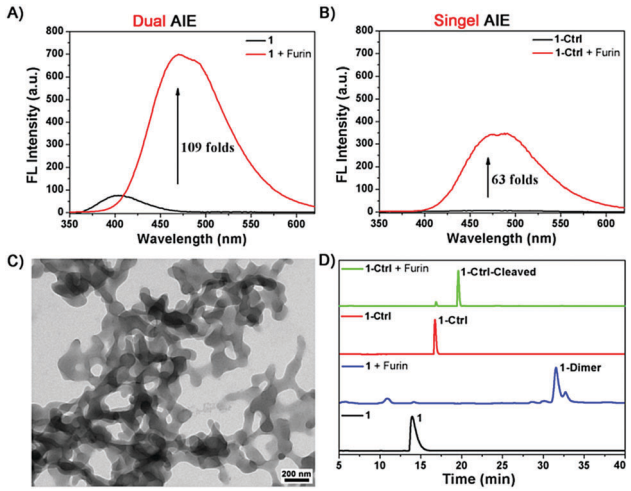

Fig. 2 (A) Fluorescence spectra of 100 μM **1** (black) and 100 μM **1** incubated with 1 nmol U^{-1} furin at 37 °C for 4 h in furin buffer (red). (B) Fluorescence spectra of 100 μM **1-Ctrl** (black) and 100 μM **1-Ctrl** incubated with 1 nmol U^{-1} furin at 37 °C for 4 h in furin buffer (red), respectively. Excitation wavelength: 320 nm. (C) TEM image of **1-NPs**. (D) HPLC trace of 100 μM **1** (black), a mixture of 100 μM **1** incubated with 1 nmol U^{-1} furin at 37 °C for 4 h (blue), 100 μM **1-Ctrl** (red), and **1-Ctrl** incubated with 1 nmol U^{-1} furin at 37 °C for 4 h (green).

addition of 1 nmol U^{-1} furin and 4 h incubation at 37 °C, we observed the fluorescence of **1** was turned on and its emission intensity at 470 nm increased approximately 109 folds (intensity: 699.9 *vs.* 6.4) (Fig. 2A). Interestingly, when **1-Ctrl** was also subjected to furin cleavage, we observed its fluorescence emission at 470 nm increased about 63 folds after furin addition (intensity: 335.2 *vs.* 5.3) (Fig. 2B). This was due to the single AIE effect of **1-Ctrl** after furin cleavage. HPLC analysis indicated that, besides a small amount of the reduction product of **1** by TCEP (*i.e.*, **1-Red**), only the condensation product **1-Dimer** but not the active intermediate **1-Cleaved** appeared on the HPLC trace (Fig. S15B in the ESI†), suggesting that the condensation was much faster than the aggregation of **1-Cleaved**. Therefore, we deduced that, compared with **1-Ctrl**, the 1.7-fold (109/63) additional emission enhancement at 470 nm of **1** resulted from the furin-controlled aggregation of **1-Cleaved** followed by further aggregation of the condensation product of **1-Dimer** (*i.e.*, dual AIE). While **1-Scr** was impervious to furin, its fluorescence emission at 470 nm did not show obvious enhancement after furin addition, as expected (Fig. S14A in the ESI†).

UV-vis spectroscopy, dynamic light scattering (DLS), and transmission electron microscopy (TEM) were used to verify the formation and characterize the aggregates obtained. The increased UV-vis absorptions from 500 nm to 700 nm (as a result of light scattering) of **1** and **1-Ctrl** after incubation with furin revealed the formation of aggregates in their respective solutions (Fig. S16 in the ESI†), which indicated the above emission enhancements of **1** and **1-Ctrl** resulted from their respective AIE effects. DLS measurements showed that the average hydrous dynamic diameters of the aggregates of **1** (*i.e.*, **1-NPs**) and **1-Ctrl** (*i.e.*, **1-Ctrl-NPs**) were about 190.1 nm and 138.7 nm, respectively (Fig. S17 and S18 in the ESI†). The TEM image of **1-NPs** indicated that the aggregates have an average diameter of 95.0 ± 5.6 nm (Fig. 2C and Fig. S19 in the ESI†).

To chemically validate that above dual AIE effects of **1** were induced by furin-controlled condensation while the single AIE effect of **1-Ctrl** was induced by furin-cleavage, we directly injected the above two incubation mixtures into a HPLC system and collected the peaks for matrix-assisted laser desorption/ionization (MALDI) mass spectroscopy analyses. As shown in Fig. 2D, a new peak at a retention time of 31.5 min, whose mass was identical to that of **1-Dimer** (Fig. S20 in the ESI†), appeared in the HPLC trace of the reaction mixture of **1**. This in principle testified our hypothesis of the furin-controlled dual AIE of **1**, as shown in Scheme 1. The enzymatic parameters K_{cat} and K_{cat}/K_m of furin towards **1** were calculated to be 7.84 min^{-1} and 0.047 μM^{-1} min^{-1}, respectively (Fig. S21 in the ESI†). The HPLC trace of the reaction mixture of **1-Ctrl** showed a main peak at a retention time of 19.7 min (Fig. 2D), whose mass agreed with that of **1-Ctrl-Cleaved** (Fig. S22 in the ESI†), suggesting that the emission enhancement of **1-Ctrl** was induced by the furin-cleavage single AIE effect. The HPLC trace of the mixture of **1-Scr** incubated with furin only showed the reduction product of **1-Scr** by TCEP in the furin buffer (*i.e.*, **1-Scr-Red**) (Fig. S14B in the ESI†), echoing that **1-Scr** did not possess the AIE effect.

After *in vitro* investigation of the specific dual AIE characteristics of **1**, we then applied **1** for enhanced fluorescence imaging of furin activity in living cells. Different from the *in vitro* studies, we used 5 μM of the probes for the cell imaging experiments. Before that, cytotoxicities of **1**, **1-Scr**, and **1-Ctrl** on furin-overexpressing MDA-MB-468 cells were investigated. The 3-(4,5-dimethylthiazol-2-yl)-2,5-diphenyltetrazolium bromide (MTT) assay indicated that, after being incubated with **1**, **1-Scr**, or **1-Ctrl** at 37 °C, more than 90% of the cells survived up to 8 hours at a compound concentration up to 40 μM, respectively (Fig. S23 in the ESI†), suggesting that a compound concentration of 5 μM is safe for cell imaging. Similarly, the minimum DMSO concentration in Dulbecco's Modified Eagle Medium (DMEM) to ensure a total solubility of **1** in the medium was tested before the probe was applied for cell imaging. The transmittance spectra of **1** in DMEM containing different concentrations of DMSO indicated that 1% was the minimum DMSO concentration for **1** to be totally dissolved (Fig. S24 in the ESI†). To overcome the interference from intracellular Cys and warrant the condensation of **1** for the aggregation of **1-NPs** inside cells,[23] we used 50 μM **C** (*i.e.*, Ac-Arg-Val-Arg-Arg-Cys(StBu)-Lys-CBT, see Scheme S2, ESI†) to co-incubate with 5 μM **1** (or **1-Scr** or **1-Ctrl** as well) for the cell imaging experiments. Time course cell imaging indicated that, while 5 μM **1** was nonfluorescent in the culture media (t = 0 min), the fluorescence of the cells gradually turned on and reached its intensity plateaus after 60 min (Fig. S25 in the ESI†), suggesting that the uptaken **1** was totally converted to **1-NPs** by the intracellular furin. We thus chose the incubation time of 60 min for the following comparative cell imaging studies.

After the MDA-MB-468 cells were incubated with 5 μM **1**, **1-Scr**, or **1-Ctrl**, together with 50 μM **C** for 60 min at 37 °C, the cells were washed with PBS three times prior to imaging, respectively. As shown in Fig. 3 (statistic of the FL intensity is

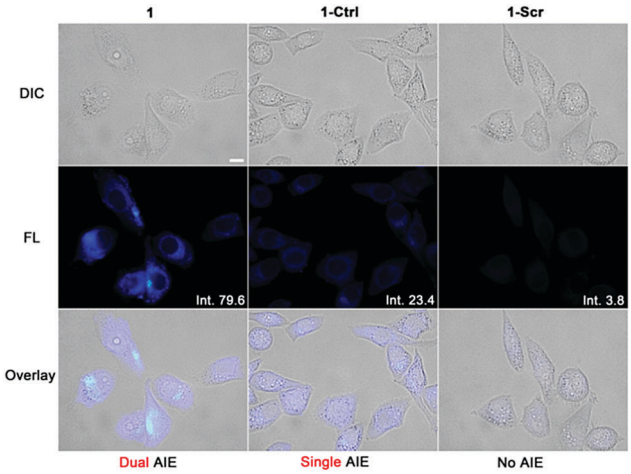

Fig. 3 Differential interference contrast images (top row), fluorescence images (middle row, DAPI channel), and merged images (bottom row) of MDA-MB-468 cells incubated with 5 μM **1** (left column), **1-Ctrl** (middle column), or **1-Scr** (right column) co-incubated with 50 μM **C** in a serum-free medium for 60 min at 37 °C, washed with PBS for three times prior to imaging, respectively. All images have the same scale bar: 10 μm.

shown in Fig. S26 in the ESI†), the cells treated with **1** had the highest FL emission intensity (mean intensity: 79.6 ± 16.9), while the emission of those cells treated with **1-Ctrl** was much lower (mean intensity: 23.4 ± 4.6) and those cells treated with **1-Scr** had the lowest emission intensity (mean intensity: 3.8 ± 1.3). These results indicated that, compared with **1-Scr**, the single AIE effect of **1-Ctrl** enhanced the FL of TPE fluorogen 6.2 folds (23.4/3.8) for cell imaging, as expected. Nevertheless, our fantastic dual AIE probe **1** additionally enhanced the FL of single AIE probe **1-Ctrl** 3.4 folds (79.6/23.4) for the best cell imaging. To verify that the above strongest fluorescence intensity from **1**-incubated cells resulted from the furin-controlled dual AIE effect as proposed in Scheme 1, we pretreated the cells with a furin inhibitor II (H-(D)Arg-Arg-Arg-Arg-Arg-Arg-NH_2) at 500 μM for 30 min before incubating the cells with 5 μM **1** and 50 μM **C**. Compared with **1**-treated cells, FL signals of the inhibitor-treated cells dramatically decreased (Fig. S27 in the ESI†). Collectively, the above results suggest that our dual AIE probe **1** can be used for enhanced FL sensing of furin activity in living cells.

In conclusion, by integrating a biocompatible condensation reaction with the AIE properties of a TPE fluorogen, we rationally designed a "smart" probe **1** for the furin-controlled dual aggregation of the TPE molecule and applied **1** for enhanced fluorescence sensing of furin activity *in vitro* and in living cells. *In vitro* results indicated that, compared with the single AIE probe **1-Ctrl**, the dual AIE probe **1** additionally enhanced the FL emission 1.7 fold. Living cell imaging results indicated that the FL emission of **1**-treated cells increased 3.4 fold compared with that of cells treated with the single AIE probe **1-Ctrl**. We envision that, in the near future, our "smart" strategy of enzyme-instructed dual AIE could be widely applied for sensing (or imaging) enzyme activity *in vitro* and even *in vivo* with dramatically enhanced sensitivity.

The authors are grateful to Chuanzhi Yao for his assistance in the synthesis of TPE-COOH. This work was supported by the Collaborative Innovation Center of Suzhou Nano Science and Technology, Hefei Science Center CAS (2016HSC-IU010), the Ministry of Science and Technology of China (2016YFA0400904), and the National Natural Science Foundation of China (grants U1532144 and 21675145).

Notes and references

1 C. Walsh, *Nature*, 2001, **409**, 226.
2 G. Thomas, *Nat. Rev. Mol. Cell Biol.*, 2002, **3**, 753.
3 M. Mbikay, F. Sirois, J. Yao, N. G. Seidah and M. Chretien, *Br. J. Cancer*, 1997, **75**, 1509.
4 M. Hosaka, M. Nagahama, W. S. Kim, T. Watanabe, K. Hatsuzawa, J. Ikemizu, K. Murakami and K. Nakayama, *J. Biol. Chem.*, 1991, **266**, 12127.
5 D. J. Ye, G. L. Liang, M. L. Ma and J. H. Rao, *Angew. Chem., Int. Ed.*, 2011, **50**, 2275.
6 C. Y. Cao, Y. Y. Shen, J. D. Wang, L. Li and G. L. Liang, *Sci. Rep.*, 2013, **3**, 1024.
7 Q. Q. Miao, X. Y. Bai, Y. Y. Shen, B. Mei, J. H. Gao, L. Li and G. L. Liang, *Chem. Commun.*, 2012, **48**, 9738.
8 A. Dragulescu-Andrasi, G. L. Liang and J. H. Rao, *Bioconjugate Chem.*, 2009, **20**, 1660.
9 Y. Yuan, J. Zhang, Q. J. W. Cao, L. N. An and G. L. Liang, *Anal. Chem.*, 2015, **87**, 6180.
10 R. Weissleder, C. H. Tung, U. Mahmood and A. Bogdanov, *Nat. Biotechnol.*, 1999, **17**, 375.
11 J. Zhou, X. W. Du, J. Li, N. Yamagata and B. Xu, *J. Am. Chem. Soc.*, 2015, **137**, 10040.
12 C. H. Ren, H. M. Wang, D. Mao, X. L. Zhang, Q. Q. Fengzhao, Y. Shi, D. Ding, D. L. Kong, L. Wang and Z. M. Yang, *Angew. Chem., Int. Ed.*, 2015, **54**, 4823.
13 J. Mu, F. Liu, M. S. Rajab, M. Shi, S. Li, C. Goh, L. Lu, Q. H. Xu, B. Liu, L. G. Ng and B. G. Xing, *Angew. Chem., Int. Ed.*, 2014, **53**, 14357.
14 J. Mei, Y. N. Hong, J. W. Y. Lam, A. J. Qin, Y. H. Tang and B. Z. Tang, *Adv. Mater.*, 2014, **26**, 5429.
15 J. W. Chen, C. C. W. Law, J. W. Y. Lam, Y. P. Dong, S. M. F. Lo, I. D. Williams, D. B. Zhu and B. Z. Tang, *Chem. Mater.*, 2003, **15**, 1535.
16 J. P. Xu, Y. Fang, Z. G. Song, J. Mei, L. Jia, A. J. Qin, J. Z. Sun, J. Ji and B. Z. Tang, *Analyst*, 2011, **136**, 2315.
17 M. C. Zhao, M. Wang, H. Liu, D. S. Liu, G. X. Zhang, D. Q. Zhang and D. B. Zhu, *Langmuir*, 2009, **25**, 676.
18 H. B. Shi, R. T. K. Kwok, J. Z. Liu, B. G. Xing, B. Z. Tang and B. Liu, *J. Am. Chem. Soc.*, 2012, **134**, 17972.
19 A. T. Han, H. M. Wang, R. T. K. Kwok, S. L. Ji, J. Li, D. L. Kong, B. Z. Tang, B. Liu, Z. M. Yang and D. Ding, *Anal. Chem.*, 2016, **88**, 3872.
20 G. L. Liang, H. J. Ren and J. H. Rao, *Nat. Chem.*, 2010, **2**, 54.
21 Z. Zheng, P. Y. Chen, M. L. Xie, C. F. Wu, Y. F. Luo, W. T. Wang, J. Jiang and G. L. Liang, *J. Am. Chem. Soc.*, 2016, **138**, 11128.
22 R. Huang, X. J. Wang, D. L. Wang, F. Liu, B. Mei, A. M. Tang, J. Jiang and G. L. Liang, *Anal. Chem.*, 2013, **85**, 6203.
23 Y. Yuan, L. Wang, W. Du, Z. L. Ding, J. Zhang, T. Han, L. N. An, H. F. Zhang and G. L. Liang, *Angew. Chem., Int. Ed.*, 2015, **54**, 9700.
24 Y. Yuan, H. B. Sun, S. C. Ge, M. J. Wang, H. X. Zhao, L. Wang, L. N. An, J. Zhang, H. F. Zhang, B. Hu, J. F. Wang and G. L. Liang, *ACS Nano*, 2015, **9**, 761.
25 G. D. Liang, J. W. Y. Lam, W. Qin, J. Li, N. Xie and B. Z. Tang, *Chem. Commun.*, 2014, **50**, 1725.

